Lattice Defects and Mechanical Behaviour of Quartz SiO2

J. Doukhan

J. Phys. III France **5** (1995) 1809–1832 NOVEMBER **1995**, PAGE 1809

Classification
Physics Abstracts
61.70E — 62.20F — 62.50

Overview Article

Lattice Defects and Mechanical Behaviour of Quartz SiO_2

J. C. Doukhan

Laboratoire Structure et Propriétés de l'Etat Solide, (associated CNRS 234), Université Sciences et Technologies de Lille, 59655 Villeneuve d'Ascq cedex, France

(Received 16 June 1995, accepted 28 July 1995)

Abstract. — Quartz has the chemical composition SiO_2. It is an abundant mineral in the Earth crust and its mechanical properties govern the rheological behaviour of a number of crustal rocks. Quartz is also a material widely used in industry (resonators, filters ...) owing to its remarkable piezoelectric properties. Very small amounts of water in the quartz lattice dramatically affect its mechanical properties. The mechanical strength of "wet" quartz is at least 10 times lower than that of "dry" quartz. This effect of water on quartz has been called hydrolytic weakening. The piezoelectric performances of resonators are also dramatically reduced by the presence of amounts of water as small as [H]/[Si] $\approx$ 300 at. ppm. In order to get better performances, crystal growers have investigated the grown-in lattice defects (dislocations, twins, occurrence of water and other chemical impurities) and their influence on piezoelectric performances. The community of mineral physicists have also investigated the lattice defects in quartz, especially dislocations, and the physical factors influencing their mobility. They have also investigated the behaviour of quartz under extreme dynamic pressure; this situation corresponds to shock waves generated by the impact of meteorites on the Earth's surface. The aim of this article is to review the mechanical behaviour of quartz under various thermomechanical conditions and the role of the impurity "water" on the relevant physical properties of quartz.

1. Introduction

α-quartz is the stable crystalline phase of silica SiO_2 at ambient conditions; it is rhombohedral with a space group $P3_121$ or $P3_221$ depending on its chirality (right-handed or left-handed three fold axis). Quartz is at a time an abundant mineral in the Earth crust and a material widely used for its piezoelectric properties (resonators). Very pure quartz is extremely strong, even at high temperature, but small amounts of water dissolved in its lattice render it much more ductile. This hydrolytic weakening effect was discovered by Griggs and Blacic in 1965 [1–3]. This solved the apparent paradox to which the mineral physicist's community was faced during more than one decade. Indeed in laboratory experiments, natural, gem quality quartz crystals (i.e. without water or dry quartz) exhibited a very high strength, even at high temperature

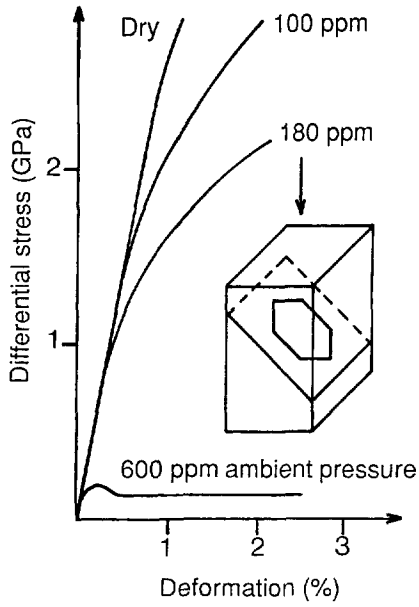

Fig. 1. — Stress-strain curves for dry (natural) and wet synthetic quartz with [H]/[Si] = 100, 180 and 600 at. ppm. Compression orientation at 45° to **a** and **c**, (often called O^+); constant strain rate $\dot{\epsilon} = 10^{-5}$ s^{-1}

and under high confining pressure and differential stress [4–7]. By contrast, in quartz-bearing rocks there is abundant microscopic evidence that quartz has flowed extensively and is weaker than other minerals such as feldspars, under most conditions occurring in the Earth's crust, i.e. at moderate temperature $\leq$ 700 °C, confining pressure $\leq$ 700 MPa, and differential stress $\leq$ 200 MPa.

Griggs and Blacic also showed that some synthetic quartz are "wet" and ductile under moderate stress and that natural (dry) quartz can be hydrolytically weakened (i.e. become ductile) in the presence of water. The strength of wet crystals is at least one order of magnitude lower than the one of natural crystals deformed in dry conditions (Fig. 1). Water contents as low as 0.005 weight % ([H]/[Si] $\approx$ 300 at. ppm) induce the weakening effect, and these wet quartz can be plastically deformed at moderate temperature ($\leq$ 500 °C) without confining pressure [8–12]. Griggs and Blacic postulated that the weakening effect stems from the hydrolysis of the strong Si-O-Si bonds by water molecules following the reaction

$$\mathrm{Si-O-Si + H_2O \Rightarrow Si-OH- \; - \; -HO-Si} \qquad (1)$$

where the broken line between the H atoms represents a weak bond. An enhanced glide mobility of the dislocations results. They also suggested that other nominally anhydrous silicate minerals should similarly be weakened by very small water contents. Although less marked than in quartz, this effect has been detected in a number of other silicate minerals like olivine $(Mg,Fe)_2SiO_4$ [13] and pyroxenes $(Mg,Ca,Fe)_2Si_2O_6$ [14]. This weakening effect is also very important in berlinite $AlPO_4$, which is not a silicate but a structural analogue of quartz [15].

A few years later, McLaren and Retchford [16] proposed a slightly different model. They suggested that the presence of water in quartz assists dislocation climb rather than dislocation

glide. Their model as well as the former one can be called localised models because only the water defects in the immediate vicinity of a dislocation core enhance its mobility in either glide or climb; in these models hydrolytic weakening implies that water defects diffuse toward the dislocation core and interact with it (assist the nucleation of jogs and/or kinks). In contrast, Hirsch [17] and Hobbs [18,19] independently proposed a delocalised model. In strong analogy with covalent semi-conductors [20,21] they assumed that dislocations in quartz are terminated in unsaturated bonds (also called dangling bonds). Randomly distributed water point defects would act like a doping and induce shallow levels in the band gap. Kinks and/or jogs, which also form localised levels in the gap, could thus trap the carriers of the shallow level. As a consequence a larger density of (charged) kinks and/or jogs would result in wet quartz, allowing a higher dislocation mobility. However the computer simulations performed by Heggie and Nylen [22,23] show that the core structures of perfect dislocations are reconstructed in quartz, i.e. the unpaired orbitals along the dislocation core rotate, overlap and form weak bonds. As a result no unsaturated (dangling) bonds are expected and no extra charged kinks or jogs should form. In contrast with the case of covalent semi- conductors, the weakening effect in quartz thus appears to be a localised effect. The mobility of the dislocations (glide and/or climb) in wet quartz must be governed by the diffusion of water point defects or at least implies that water point defects diffuse toward the dislocation cores.

Water point defects also strongly affect the performances of piezoelectric devices. Small amounts of water dramatically decrease the quality factor of quartz resonators. Up to the sixties piezoelectric components were cut in natural gem quality single crystals (mostly collected in Brazil). With the development of modern electronics the need for numerous, cheap, and precise quartz resonators, filters and other piezoelectric devices has rendered necessary the mass production of large quantities of synthetic quartz. Actually more than 1,500 tons of synthetic quartz are grown every year in the world and most crystal growers estimate the piezoelectric efficiency of their crystals by measuring their concentration of O-H radicals [24–26]. In a continuous effort spent over a decade or more, crystal growers have reduced the water content of synthetic crystals. They actually produce high quality quartz (premium grade) from natural seeds (natural quartz crystals generally contain a very low dislocation density) and at a very low growth rate ($\leq$ 0.2 mm/day). This allows growth to occur at thermodynamic conditions very close to equilibrium. These modern synthetic crystals with water contents as low as [H]/[Si] $\leq$ 20 at. ppm are drier and purer than most natural gem quality quartz which most often contain small amounts of chemical impurities, especially Al. This later impurity is associated with a proton for charge compensation. This complex defect induces a severe damping of the electro-acoustic waves and decreases the piezoelectric performances of resonators. Well designed resonators carefully machined in pure synthetic quartz material have a remarkable high precision. Good time keeping quartz devices present a long time relative shift of their resonance frequency as low as 10^{-11} i.e. the uncertainty on absolute time measurement is less than 3 seconds per million year; their short time shift can be as low as 10^{-14}

2. Crystallography, Dislocations, Twins and Glide Systems

Figure 2 shows the stability fields of the various polymorphs of silica. α-quartz is stable up to 573 °C at ambient pressure. Above this temperature it transforms into β-quartz. The transition is displacive (indicated by a double arrow in Fig. 2b) and the β phase is non quenchable. The rhombohedral structure of α-quartz was elucidated by Braggs and Gibbs in 1926 [27]; its Bravais lattice is hexagonal and the four index notation of Miller-Bravais is used below for both the direct and the reciprocal space [28,29]. The unit vectors of the primitive cell are at room conditions $\mathbf{a} = 0.4921$ nm and $\mathbf{c} = 0.5400$ nm (review of recent determinations

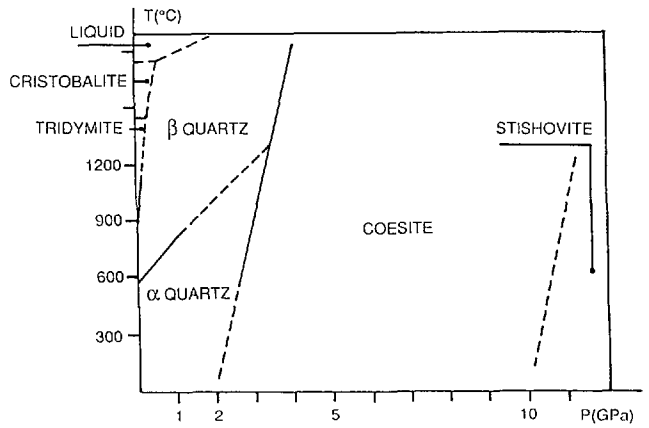

Fig. 2. — a) Stability fields of the various silica polymorphs. b) Phase transformations at ambient pressure.

in Ref. [30]). The Si and O atoms form a tridimensional network of SiO_4 tetrahedra sharing their four corners. Because of the marked covalent character of the Si-O-Si bonds the quartz structure has no plane with weak bonds into which dislocations would easily glide. Figure 3 is a simplified representation of the crystal structure. Only the Si atoms and the strong Si-Si bonds *via* an oxygen atom are reported (bars). The O atoms (not represented) lie approximately in the middle of the bars. Among the numerous twin laws of quartz [31] two are frequently observed, the Dauphiné and Brazil twins. Dauphiné twinning corresponds to a π rotation around the three fold screw axis **c**. It is an electric poison for piezoelectric devices because the polarisation vector parallel to **a** is reversed in the twinned domains. Dauphiné twin boundaries can have any orientation, but they most often run parallel to the prismatic planes $\{10\bar{1}0\}$. In the high temperature polymorph β-quartz, **c** becomes a sixfold axis and the π rotation around **c** becomes a symmetry operation of the structure; therefore Dauphiné twins disappear above the $\alpha \rightarrow \beta$ transition. Dauphiné twins often form during cooling from high temperature. At the $\beta \rightarrow \alpha$ transition, they occur as low temperature variants. Brazil twinning results from the change of the enantiomorphous or chiral character of the threefold screw axis **c** (left-handed $\leftrightarrow$ right handed); these twins do not vanish at the $\alpha \leftrightarrow \beta$ transition. Both types of twins have the peculiarity of keeping unchanged the Bravais lattice (no extra spots on diffraction patterns), only the positions of the atoms in the unit cell change. Therefore such twins do not look like mechanical twins and are not expected to form by plastic deformation like the $\{11\bar{2}2\}$ twins in usual hexagonal structures like zinc for instance.

In most crystals the Burgers vectors of the mobile dislocations are the shortest lattice repeats of the structure. In α-quartz the lattice parameters **a**, **c** and **a**$\pm$**c** are the shortest lattice repeats and all three have been characterized as Burgers vectors of either as-grown dislocations or dislocations induced by natural or experimental deformation. A number of techniques have

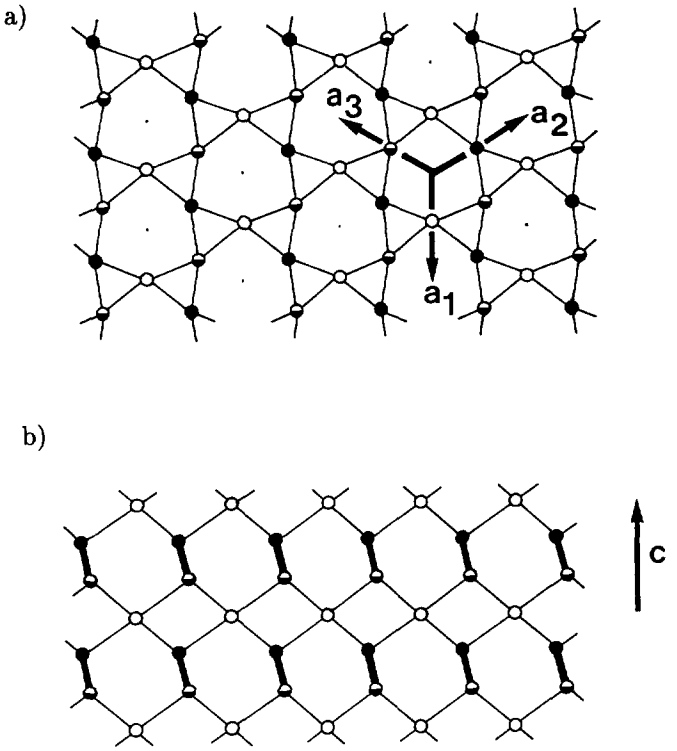

Fig. 3. — Structure of α-quartz projected on a) basal plane (0001). b) On prismatic plane $(2\bar{1}\bar{1}0)$. Si atoms at level $c = 0$ are represented by an open circle; the ones at $c/3$ by a half filled circle and the ones at $2c/3$ by a filled circle. Their atomic positions in the unit cell are $u\mathbf{a}_1$, $u\mathbf{a}_2 + \mathbf{c}/3$, and $u\mathbf{a}_3 + 2\mathbf{c}/3$ with $u = 0.465$ at room temperature. Thick bars on b) indicate that two different bonds have the same projection (they connect a given atom to two other ones which appear on the projection at the same place).

been used for characterizing them: etch pitting for determining their densities and their glide planes [32, 33], X-ray (Lang) topography [34–36], and Conventional Transmission Electron Microscopy (CTEM) [11, 37–39]. Characterizations by CTEM are rendered difficult by the sensitivity of the material to electron beam (it rapidly amorphises). A few unambiguous Burgers vectors determinations were performed by using the criterion of no contrast in two beam conditions for $\mathbf{g} \cdot \mathbf{b} = 0$ ($\mathbf{g}$ = diffraction vector, $\mathbf{b}$ = Burgers vector). These results have recently been confirmed by Large Angle Convergent Beam Electron Diffraction (LACBED) [39], a technique necessiting a very weak intensity. Trépied and Doukhan [40] suggested on the basis of CTEM observations that **a** dislocations produced by experimental deformation in wet synthetic quartz are slightly dissociated in either the basal (0001) or a prismatic $\{10\bar{1}0\}$ plane following the reaction

$$\mathbf{a} \rightharpoonup 1/2\mathbf{a} + 1/2\mathbf{a} \qquad (2)$$

They also proposed a crystallographic model for low stacking fault energy: all the SiO_4 tetrahedra on both sides of the fault must still share their four corners and keep mutual orientations close to the ones in the perfect crystal. Dissociation of **a** dislocations in the basal plane fulfil this criterion only in the case of a zonal dissociation, i.e. a dissociation extending in three

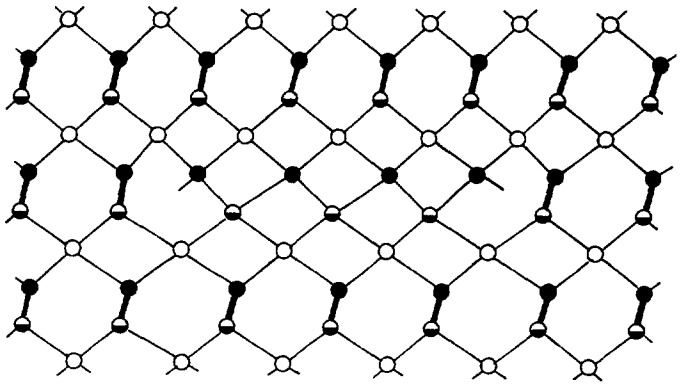

Fig. 4. — Model of zonal dissociation of a **a** dislocation in the basal plane, after [12].

adjacent basal layers (Fig. 4). Further investigations by Cherns *et al.* [41] by High Resolution Transmission Electron Microscopy (HRTEM) on naturally deformed quartz did not reveal, however, any dissociation. More recently Cordier and Doukhan [42] observed widely dissociated **a** and $\mathbf{a} \pm \mathbf{c}$ dislocations with dissociation widths > 1 μm in a synthetic quartz with a low water content experimentally deformed under high differential stress. They obtained by LACBED unambiguous characterizations of the partial Burgers vectors (these results are independent of the possible anisotropy of the crystal). **a** basal dislocations are dissociated following the reaction proposed by Trépied and Doukhan (Eq. (2)). $\mathbf{a} \pm \mathbf{c}$ dislocations also dissociate into two collinear partials with equal Burgers vectors $1/2(\mathbf{a} \pm \mathbf{c})$. This comforts the crystallographic model of zonal dissociation for **a** dislocations. The criterion is also satisfied for the stacking faults in $\{10\bar{1}0\}$ prismatic planes associated with $1/2(\mathbf{a} \pm \mathbf{c})$ partial dislocations. Altogether these observations show that the amount of water and the deformation parameters T, P, and especially the intensity of the applied differential stress can change the fine core structure of the mobile dislocations. The mobile dislocations would be any type of perfect dislocations (Burgers vectors **a**, **c**, and $\mathbf{a} \pm \mathbf{c}$) in very wet crystals which can be plastically deformed without confining pressure and at moderate stress level. In contrast, in quartz with a low water content which can be deformed only under large confining pressure and large differential stress, only the dislocations with the lowest stacking fault, will be able to widely dissociate, would have an appreciable mobility and the number of active glide systems would be severely reduced. In quartz with low OH content the mobility of dislocations thus seems to parallel their ability to dissociate.

3. Solubility and Diffusivity of Water in Quartz

Although the Czochralski process (slow solidification of the molten phase) is widely used for materials like silicon for instance, it cannot be used to grow synthetic quartz because of the occurrence of high temperature polymorphs. α-quartz is thus synthesised by hydrothermal growth at moderate temperature and pressure (typically 360 °C, 150 MPa) in large autoclaves separated in two regions by a small aperture. The high temperature region contains a SiO_2 saturated aqueous solution (nutrient) and the lower temperature region contains the growing crystals. NaOH or Na_2CO_3 is often added to the nutrient in order to increase the solubility of SiO_2. It is not surprising that in such conditions the first synthetic crystals produced in the sixties contained a lot of water. This water content is currently detected and

quantitatively measured by Infrared Absorption Spectroscopy (IAS) in the wave number range 4000-2500 cm^{-1} [43–45]. Water contents as large as [H]/[Si] = 3000 at. ppm have been measured in crystals grown some thirty years ago or so. In contrast recently grown quartz are much dryer with water contents below the detectability limit of the technique ($\leq$ 20 at. ppm). Many growth experiments have shown that the first crystals synthesised in the sixties were supersaturated because of too high growth rates which led to growth in non equilibrium conditions. Most of the water occurs in these crystals under the form of very tiny fluid inclusions (10 to 100 nm in diameter) which were first detected by Transmission Electron Microscopy (TEM) by McLaren *et al.* [46]. The true solubility of water in quartz under the form of randomly distributed point defects must be quite low at the standard (T, P) growth conditions. Substitutional Al^{3+} impurities associated with a proton for charge balance have also been detected by Electron Spin Resonance (ESR) and IAS [47]. It is unlikely that these impurities often noted Al-OH centres play an important role in hydrolytic weakening, as their diffusivity is expected to be extremely low; in the following they are not considered.

The possibility of introducing water point defects in an initially dry quartz (diffusional uptake) has been carefully tested at high temperature and high confining pressure [44, 48–51]. No significant increase of the water content were observed. Either the solubility or the diffusivity of these point defects is very low. One must thus actually assume that in the original weakening experiments of Blacic and Griggs, water was introduced in the samples along their numerous fractures generated by the large confining pressure.

The equilibrium solubility of water point defects in quartz has been tentatively computed by several authors [12, 52–57]. All these computations are grossly based on the same hypotheses and can be schematically summarized as follows. One considers a thermodynamic system constituted of a reservoir of pure water with a quartz crystal immersed in it. For a given model of water point defects (substitutional or interstitial) the Gibbs energy of the system is computed as a function of the relevant thermodynamic variables, T, P, and the concentration of water point defects. This Gibbs energy is then minimised *versus* the concentration of point defects at given T and P. This yields the theoretical equilibrium solubility of point defects $c(T, P)$. This function contains, however, unknown parameters, the values of which can be determined by equating the theoretical $c(T, P)$ function to known (or assumed to be known) values of this equilibrium concentration at different sets of (T, P) conditions. For instance the concentration of OH in premium grade quality quartz is of the order of 20 at. ppm and is assumed to be an equilibrium value. Except for Haggon *et al.* [58] who assume that water enters in quartz under the form of interstitial molecules (which preferentially diffuse along the **c** channels), all other authors assume that water dissolves in quartz under the form of substitutional defects noted $(4H)_{Si}$. Such a defect is formed by the substitution of a SiO_2 group by two water molecules or equivalently the substitution of a Si atom by 4Hs. This defect is equivalent to the $(4H)_{Si}$ hydrogarnet defect already characterized in grossular garnet [59–61]. In quartz $(4H)_{Si}$ defects have been experimentally characterized by ESR [62, 63]. They have also been shown to be related to hydrolytic weakening [64]. The computation of the equilibrium solubility of water defects is schematically done as follows. Let $g(T, P)$ be the Gibbs energy of a water molecule in the water reservoir of the system considered above. Incorporating 2 water molecules in the initially dry crystal as a substitutional point defect increases the Gibbs energy of the crystal by G_f (G_f = Gibbs energy of formation of the defect) and decreases the Gibbs energy of the water reservoir by $2g(T, P)$. Incorporating $2n$ water molecules in the crystal leads to a variation of the Gibbs energy of the system

$$\Delta G = +nG_f - 2ng(T, P) - TS_{mix} \tag{3}$$

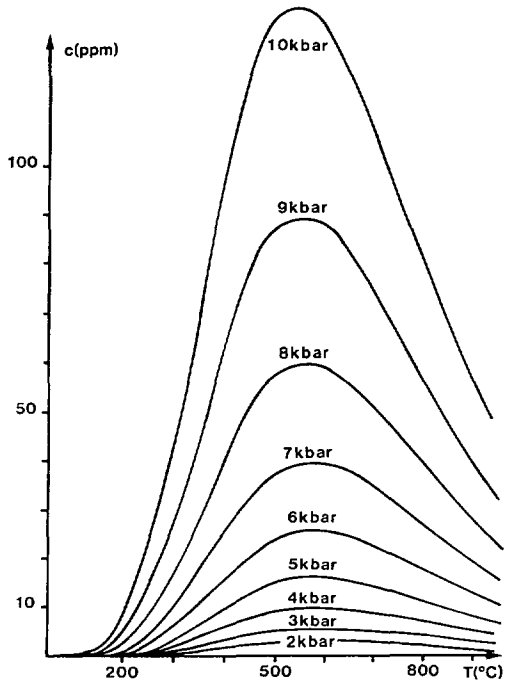

Fig. 5. — Equilibrium solubility $c(T, P)$ of $(4H)_{Si}$ substitutional defects in quartz after [52].

where S_{mix} is the usual mixing entropy associated with the formation of n such point defects in a crystal lattice with N possible sites for them.

$$S_{mix} = k\mathrm{Ln}\frac{(N+n)!}{n!N!} \tag{4}$$

The equilibrium atomic concentration of $(4H)_{Si}$ defects $c(T, P)$ immediately results from the minimisation of ΔG *versus* n at fixed T and P

$$c(T, P) = \exp\frac{-G_f + 2g(T, P)}{kT} \tag{5}$$

The variation with T and P of the Gibbs energy $g(T, P)$ of pure water is well known up to quite large T and P values [65–67]. However it is clear that the fluid in equilibrium with the crystal at high T and P must not be pure water but an aqueous solution appreciably enriched in silica. Using the $g(T, P)$ data of pure water is thus a highly simplified approximation. One also assumes that the formation Gibbs energy $G_f = H_f - TS_f$ is such that H_f and S_f are constant. In these conditions, only two experimental values of the solubility are necessary for fully determining the equilibrium solubility function $c(T, P)$. Depending of the choice of the calibrations values various $c(T, P)$ functions are obtained which lead to solubilities varying from H/Si $\approx$ 10 to a few hundred at. ppm at high T and P values. Although they substantially differ, all computations predict a dramatic increase of $c(T, P)$ with P, at least at moderate temperature. For example, Figure 5 shows the variation of $c(T, P)$ estimated by Doukhan and Paterson [52]. Oxygen fugacity has also been reported to affect the ductility of quartz [55,68]. We assume, however, that this phenomenon stems from the fact that, like P_{H_2O}, P_{O_2} must

affect the solubility of the water point defects and this effect could be estimated by standard thermodynamic computations.

There have been much less investigations of the diffusivity of water point defects in quartz. Some indirect measurements [46, 55, 57] suggest an apparent diffusion coefficient at ambient pressure

$$D = D_0 \exp(-E/RT)$$

$$\text{with } D_0 = (10 \pm 2)10^{-11} \text{ m}^2 \text{ s}^{-1} \text{ and } E = (95 \pm 10) \text{ kJoule mole}^{-1} \quad (6)$$

This law was determined by studying the nucleation and growth of tiny water precipitates in a wet quartz into which all the water was initially dissolved as randomly distributed $(4H)_{Si}$ point defects. The microscopic state of water dispersion in the bulk of a quartz crystal, molecular water in tiny fluid inclusions or $(4H)_{Si}$ point defects can be determined by Near Infrared Absorption Spectroscopy (NIAS) in the wave number range 7000-4500 cm^{-1} Indeed it has been experimentally shown that both, molecular water in fluid inclusions and $(4H)_{Si}$ point defects, contribute to the same large absorption band in the 3 cm^{-1} band. This band results from the stretching and bending modes of both types of water. Conventional IAS thus yields the total water content of the investigated specimen by measuring the integral absorbency between 4000 and 2500 cm^{-1}. In contrast NIAS in the range 7000-4500 cm^{-1} allows molecular water and $(4H)_{Si}$ point defects to be distinguished. The technique has been successfully applied to the study of glasses [69–71] and various forms of silica [72, 73] including quartz [44, 45]. The absorption band centred on 4500 cm^{-1} results only from the vibration modes of isolated OH radicals (i.e. of Si-OH groups) while the one at 5200 cm^{-1} results from a combination of the bending and stretching vibration modes of H_2O molecules. It is thus possible to differentiate molecular water from point defects. Unfortunately the technique is much less sensitive that conventional IAS. Much thicker samples (up to 20 cm long for low OH content material) have to be used, leading to mean concentrations over quite large volumes.

The annealing at temperature T and at ambient pressure (i.e. at conditions corresponding to a very low equilibrium solubility of the water point defects) of a crystal in which all its initial water content was practically under the form of point defects must lead to the precipitation of molecular water. Tiny water bubbles (10 to 50 nm diameter) are effectively detected by TEM in this annealed material and their mean distance X is easily measured. By equating this quantity X to twice the random walk distance of the point defects during the annealing process one gets an estimate of the diffusion coefficient D of the water point defects

$$X/2 = \sqrt{2Dt} \text{ or } D = \frac{X^2}{8t} \quad (7)$$

where t is the duration of the annealing. It is to be mentioned that this D value is only an apparent diffusion coefficient. As soon as the nuclei of the precipitates are formed the measured activation energy corresponds to a complex sequential process consisting of (i) diffusion of the point defect over a distance of the order of $X/2$ and (ii) condensation of this defect in the precipitate. It is not impossible that an Ostwald ripening process also occurs at some stage of the annealing experiment. When many tiny precipitates with various sizes have nucleated, the Ostwald ripening consists in the diffusion of water point defects from the smaller precipitates toward the larger ones. The larger precipitates thus grow at the expense of the smaller ones which progressively disappear (but new ones continuously nucleate). Taking into account this Ostwald ripening phenomenon, the experimentally measured activation energy of our apparent diffusion coefficient D would correspond to a still more complex sequence consisting of (i) dissolution of the point defect in the quartz matrix in the immediate vicinity of a small precipitate, (ii) migration of the defect toward the larger precipitate, and (iii) condensation

of the point defect in this larger precipitate. Whatever the exact process associated with the measured diffusion coefficient D (Eq. (6)), we can assume that it is not markedly different from the one involved in water assisted deformation (hydrolytic weakening) when water point defects diffuse toward dislocation cores and are absorbed by them.

4. Water Assisted Deformation of Wet Quartz

Since the experiments of Griggs and Blacic, a vast literature has been published on the rheological behaviour of quartz. In the case of wet synthetic quartz a simple comparison of the experimental data published so far (stress- strain curves at given T and $\dot{\epsilon}$ for instance) gives the impression that the behaviour of synthetic quartz is not well reproducible. For a better understanding of these results, it may be useful to distinguish a few groups of experiments.

4.1. Experiments Performed on Dry Quartz. — This material is very strong, even at high temperature. As a consequence, deformation tests have to be performed under confining pressure in order to avoid fracturing. A number of constant strain rate experiments have been done in both solid and gas confining media. The experiments performed in a gas confining medium are generally done at $P = 300$ MPa [74–76] but Baldermann [77] worked at pressures up to 500 MPa. In solid confining medium larger pressures up to 1500 MPa can be reached [1–6, 74]. The Griggs-type deformation apparatus induces, however, more fracturing in those very strong and brittle specimens. Below $\approx$ 700 °C no plastic deformation can be induced in dry quartz, even at very high differential stress. Above this temperature the stress-strain curves show a limited amount of plasticity accompanied by a large strain hardening (see Fig. 1). The few TEM observations done on those samples reveal that most of the deformation results from fracturing. One observes restricted areas with a large density of dislocations while other regions are dislocation free. Amorphous silica and coesite have also been observed [78] as well as **a** dislocations widely dissociated in the basal plane [79]. In the experiment performed at the highest temperature (1300 °C) Doukhan and Trépied [12] detected a dislocation activity only at crack tips where the differential stress is increased by the stress concentration factor. Straight dislocations with Burgers vectors **a** and **a**$\pm$**c** were characterized. They are confined in their glide plane and present preferential directions parallel to simple crystallographic directions (Fig. 6). It thus appear that even at temperature as high as 0.80 T_M (T_M = melting temperature of silica $\approx$ 2000 K) deformation appears to be controlled by a Peierls regime and dislocation climb is not activated. The activation energy associated with the nucleation of kinks was independently estimated by Doukhan and Trépied [12] on the basis of their TEM observations and by Heggie [80] by computer simulations. Both find an order of magnitude of 5 eV. As no dislocations in climb configuration are observed the activation energy associated with dislocation climb must be larger than that.

4.2. Experiments Performed on Wet (Synthetic) Crystals. — Synthetic crystals grown in the sixties are generally rather wet with [H]/[Si] typically of the order of 1,000 at. ppm and almost all their OHs occur under the form of molecular water in tiny fluid inclusions (detected by TEM on as-grown, untreated crystals). Such crystals are very ductile and mechanical tests can be performed without confining pressure. A number of deformation experiments have been done at atmospheric pressure and at various temperatures in usual constant strain rate machines or in dead load creep apparatuses [8–10, 12, 38, 81–83]. Experiments on single crystals or quartz aggregates were also performed with confining pressure for comparison with dry quartz [74, 76, 84–87]. In a number of cases the deformation microstructures were investigated by TEM. The results (stress-strain curves and dislocation microstructures) are,

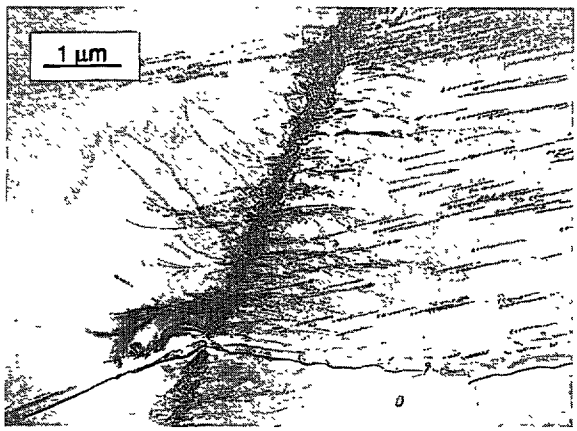

Fig. 6. — Dry quartz deformed at $T = 1300$ °C, $P = 300$ MPa in a gas medium apparatus. Dislocation activity is confined to crack tips. No dislocation climb is observed. The extended horizontal defect (bottom) is a narrow lamella of amorphous silica.

however, hardly comparable. It is now clear that these apparent discrepancies stem from the state of dispersion of water which continuously changes with time as deformation proceeds. At the beginning of a deformation experiment the specimen contains a high density of very tiny fluid inclusions with a few tens to one hundred nm diameter. Due to the Ostwald ripening phenomenon, the fluid inclusion distribution evolves toward a lower density of larger water bubbles. The growth of the larger fluid inclusions implies that SiO_2 matter is removed from the bubble surfaces in order to relax their inner pressure. This is the origin of the strong driving force which activates the diffusion of Si and O atoms from growing bubbles (sources) toward neighbouring dislocations (preferential sinks). As a result these dislocations climb. Superimposed to the applied stress, the Ostwald ripening-induced driving force may progressively become the prominent factor governing the plastic behaviour of wet quartz [83]. The first important aspect of hydrolytic weakening in rather wet synthetic quartz can thus be described as a dramatic enhancement of dislocation climb, but dislocation glide is also dramatically enhanced. This is the second aspect of hydrolytic weakening which results from the decrease of the nucleation energy (and of the propagation energy) of elementary kinks by the water point defects in the dislocation cores. All types of dislocations (Burgers vectors $\mathbf{a}$, $\mathbf{c}$ and $\mathbf{a} \pm \mathbf{c}$) can be activated i.e. weakening affects all glide systems. The dislocation microstructures observed by TEM show a marked evolution with time and amount of strain. They progressively change from dislocation configurations typical of a glide controlled Peierls regime at the beginning of the deformation (straight dislocations confined in their glide plane and parallel to simple crystallographic directions, Fig. 7a) to recovery microstructures at larger deformations (curved dislocation segments, numerous junctions and irregular subgrain boundaries, Fig. 7b). This change is detected even in specimens deformed at the lower temperatures (700 K $\approx T_M/3$). An annealing treatment performed before deformation or a heating stage before deformation with a low temperature slope strongly affect (increase) the flow stress. The initial dislocation multiplication process also seems very specific in wet synthetic quartz. These as-grown crystals contain quite a low dislocation density (typically $\approx 10^6$ m^{-2}). A dramatic increase of this density is thus necessary at the beginning of a constant strain rate test. In materials like silicon which also have a very low initial dislocation density, this dislocation multiplication induces in imposed strain rate tests a severe increase of the flow stress which then decreases

Fig. 7. — Typical dislocation microstructures in a wet synthetic crystal ([H]/[Si] ≈ 1,000 at. ppm). Compression axis // O^+ (at 45° to the **a** and **c** directions), $T = 600$ °C, constant strain rate $\dot{\epsilon} = 5 \times 10^{-6}$ s^{-1}. a) Total strain $\epsilon \approx 2\%$, the dislocations are confined in their glide plane; they show preferred orientations parallel to simple crystallographic directions. b) Total strain $\epsilon = 10\%$, dislocations are in climb configuration, they begin to form irregular subgrain boundaries. c) Total strain $\epsilon = 0.1\%$, dislocation multiplication is homogeneous and occurs by the nucleation of small dislocation loops on the growing fluid inclusions.

in the following steady state regime (yielding phenomenon with upper and lower yield points). Similarly creep tests present a transient regime (sigmoidal creep). This dislocation multiplication process leads in silicon and similar materials to a heterogeneous dislocation density at the beginning of the deformation. Every activated Frank-Read source leads to a deformation band with a large dislocation density while other regions still are undeformed and dislocation free. In contrast in wet quartz detailed TEM investigations performed after very slight strains clearly show that the dislocation multiplication process is pervasive and homogeneous. This homogeneous dislocation multiplication in wet quartz results from the evolution of the fluid inclusions. In order to relax their inner pressure in an environment with a low dislocation density the growing bubbles nucleate small sessile dislocation loops which expend by climb

in absorbing the Si and O atoms emitted by the bubble surfaces (Fig. 7c). When the loops have reached a characteristic size (which depends on the applied stress) their screw segments cross-slip and start the glide process while their edge segments still climb and contribute to the relaxation of the inner pressure of the bubbles. It thus appear that larger the initial density of fluid inclusions, larger the strain rate is. This competition between Ostwald ripening which leads to a decrease of the density of fluid inclusions and plastic deformation can produce an inversion in the flow stress *versus* temperature curve. A given specimen tested at a series of increasing temperatures first softens as T increases, then progressively hardens at higher temperature because the density of fluid inclusions decreases.

4.3. Experiments Performed on Crystals with a Low Water Concentration

We are concerned here by crystals with typical water contents of $\approx$ 100 ppm occurring mostly as $(4H)_{Si}$ point defects. One can find in some old crystals grown in the sixties a few end regions where the water content is of this order of magnitude and is for a large part constituted of $(4H)_{Si}$ defects. This probably results from the fact that these crystals were grown in autoclaves with a poorly controlled temperature difference between the high temperature region with the nutrient and the lower temperature region with the growing crystals (this temperature difference controls the rate of silica brought to the growing crystals). At the end of the growth process, the total crystalline surface onto which the supersaturated nutrient deposits silica is much larger than at the beginning and the growth rate is appreciably reduced. The end regions can thus grow in conditions close to equilibrium leading to drier material. Crystals with a low water content have also been deliberately grown in modern autoclaves with a constant and well controlled growth rate but slightly larger (0.3 to 0.5 mm/day) than the one corresponding to thermodynamic equilibrium and minimum water content. These crystals have a strength comprised between the one of dry quartz and that of the wetter crystals considered in the previous Section. Deformation tests have to be performed under confining pressure in order to avoid fracturing.

One has to distinguish two types of deformation conditions. Either they are such that the concentration of $(4H)_{Si}$ point defects does not exceed the equilibrium solubility or the (T, P) conditions correspond to a supersaturated water content. In the later case molecular water will precipitate during the course of the deformation and the state of dispersion of water will continuously change (no steady state is obtained). All experiments performed in a gas medium apparatus correspond to this situation because the solubility of $(4H)_{Si}$ point defects remains extremely low at 300 to 500 MPa whatever the temperature. Water precipitates during deformation but this precipitation seems slower than at ambient pressure and dislocation microstructures typical of a Peierls regime extend over larger strain (or longer duration). Tiny water precipitates and dislocation climb finally become the prominent features on TEM micrographs of highly deformed samples, in strong analogy with the case of wetter crystals. Deformation in a solid medium apparatus allows larger confining pressure to be reached, up to 1500 MPa. As a general trend high confining pressure and high differential stress induce fracturing in the sample (in the original Blacic and Griggs experiments such fractures allowed hydrolytic weakening to occur in initially dry specimens deformed in wet assemblies). In addition, in these solid medium apparatuses the large friction along the mobile piston leads to less precise stress-strain curves. A few experiments have been performed at confining pressures $P = 800$ to 1200 MPa and various temperatures [42,56,57]. Samples with a water point defect concentration of 180 at. ppm are supersaturated for all the tested conditions and water precipitates.The dislocation microstructures observed by TEM are typical of recovery with pervasive

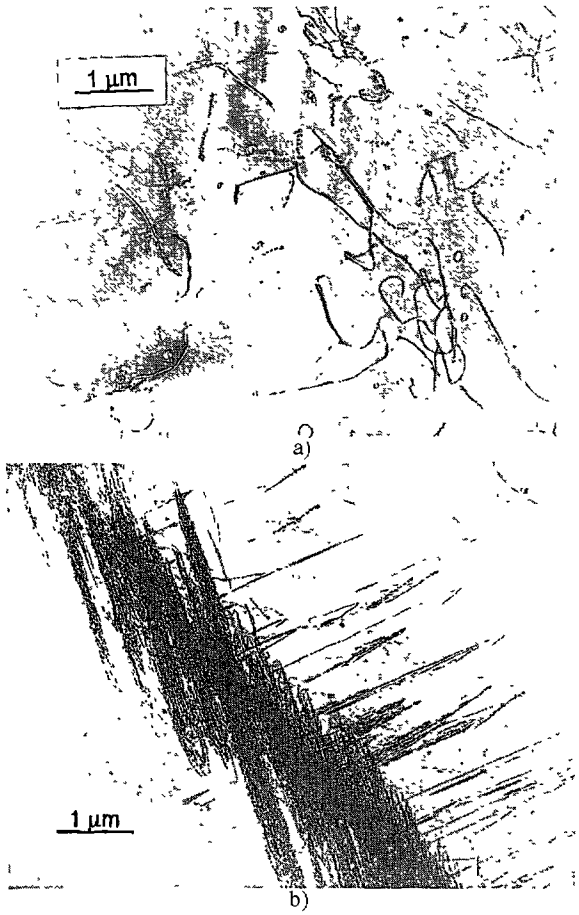

Fig. 8. — a) Dislocation microstructure typical of recovery in a crystal with [H]/[Si] $\approx$ 180 at. ppm. Compression axis // O^+. $T = 700$ °C, $P = 1000$ MPa, $\dot{\epsilon} = 10^{-6}$ s^{-1} b) Dislocation microstructure typical of a Peielrs regime in a wet quartz with [H]/[Si] $\approx$ 100 at. ppm. Deformation conditions identical to a).

climb configuration (Fig. 8a). In contrast, samples with a slightly lower concentration (100 at. ppm) tested at pressure > 1000 MPa are markedly stronger at equivalent temperatures (but still weaker than dry quartz). Their microstructures show only glide, even at the higher temperature tested $T = 900$ °C (Fig. 8b). Only glide in (0001) and $\{10\bar{1}0\}$ planes can be activated in strong similarity with what was observed in dry quartz.

Therefore in these later experiments only the weakening effect acting on the glide motion of dislocations is activated. It results from the diffusion of water point defects toward the dislocation cores where they assist the nucleation (and the propagation) of elementary kinks. In contrast with the previous case, dislocation multiplication is not homogeneous at the beginning of the deformation. TEM observations on samples with a small strain reveal a few dislocation bands separated by large regions which are dislocation free. The density of dislocation bands increases with strain and the stress-strain curves exhibit an initial parabolic stage which extends up to $\epsilon \approx 5\%$.

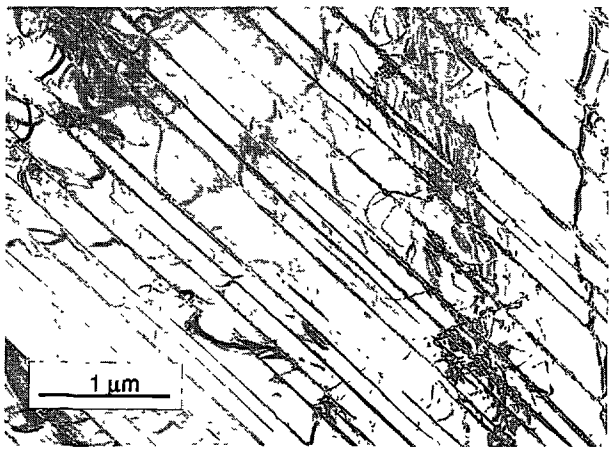

Fig. 9. — Single set of PDFs parallel to $\{10\bar{1}3\}$ in naturally shocked quartz (meteorite impact of Popigai, Russia). They are straight and narrow lamellae of dense amorphous silica.

It is remarkable that in berlinite $AlPO_4$, the structural analogue of quartz, only **a** glide is activated in the dry material while, in wet crystals with numerous tiny water bubbles, all types of dislocations are nucleated, even the ones with the unexpectedly large Burgers vector $\mathbf{a} \pm \mathbf{c}$ [38]. The atomic arrangement is practically identical in both structures and the lattice parameters are practically identical except that due to the ordering of Al and P atoms, **c** is twice larger in berlininte and is thus unexpected as a Burgers vector (and $\mathbf{a} \pm \mathbf{c}$ is still larger).

5. The Behaviour of Quartz Under Very Large Pressure

Geophysicists are interested to the behaviour of quartz submitted to strong shock waves because this situation corresponds to the deformation conditions occurring during the impact of a large meteorite colliding the Earth surface at hyper velocity (20 to 40 km/s). A number of large meteorites have hit the Earth in the two first billion years of its history. They induced in the target rocks a very strong shock compression during a very short time which in turn induced characteristic lattice defects in the target minerals. In quartz grains these shock-induced lattice defects have been found to be very resistant to subsequent metamorphic or weathering events and in a number of cases they can still be detected. In contrast with many metals and more ductile minerals, shock waves do not induce dislocation activity in quartz. This has been checked on both wet and dry quartz, with various initial dislocation densities. These materials have been experimentally shocked at various temperatures and shock pressures with high explosives. No significant increase of the dislocation density has been detected by TEM. The duration of the compression stage (a few microseconds for experimental shocks) is probably too short to allow the dislocations to propagate and multiply [88]. Shock induced defects in quartz are called Planar Deformation Features (PDF). They are experimentally generated by shock waves with peak pressures $\geq$ 15 GPa and are easily detected by optical microscopy (transmitted light). They appear as very straight and narrow contrasts parallel to a few crystallographic planes with low crystallographic indices $\{10\bar{1}n\}$ with $n = 2$ and 3 as most frequent values but $n = 1$, 4 and the basal plane (0001) are also observed. In TEM PDFs appear as lamellae typically 100 nm thick of amorphous silica (Fig. 9). The measurement of its refractive index suggests that in contrast with usual silica glass, this amorphous phase

is denser than crystalline quartz. The occurrence of PDFs in quartz grains of a rock are presently considered as the best indicator that a large meteorite impacted the rock at high velocity. PDFs can still be detected (and considered as an unambiguous impact signature) millions or even one or two billions years after the impact event. The oldest meteorite impact structure detected so far on the Earth surface (the Vredefort structure in South Africa) is more than two billions years old. In some weathered rocks which were immersed in aqueous fluids for a long time (on a geological scale, i.e. during millions years), this amorphous silica can partially or even completely recrystallize but in a number of cases there remains some PDFs or remnants which still can be unambiguously detected. It is also to be mentioned that small grains of high pressure silica polymorphs (coesite and stishovite) are also detected in impacted quartz.

Very similar straight and narrow lamellae of amorphised material running parallel to a few crystallographic planes are also detected in some other shocked silicate minerals like feldspars and pyroxenes. By analogy with the case of quartz they have been called PDFs. It is believed that all these PDFs have the same formation mechanism based on the transformation of the mineral into a denser amorphous silicate. At atmospheric pressure silicon presents in silicate minerals a fourfold coordination (SiO_4 tetrahedra). At higher pressure most silicate minerals transform into high pressure crystalline forms with six-fold coordinated Si atoms (SiO_6 octahedra). For instance the crystal structure of stishovite, the high pressure polymorph of silica, consists of a tridimensional network of edge sharing SiO_6 octahedra and this phase is $\approx 40\%$ denser than quartz. This strongly suggests that the narrow PDF lamellae in quartz would be a phase constituted by an irregular array of edge sharing SiO_6 octahedra (stishovite glass). At the very high pressure of the shock wave the stable phase of silica is stishovite but the reconstructive phase transformation quartz $\rightarrow$ stishovite is sluggish even at high temperature. In contrast the transformation crystalline quartz $\rightarrow$ amorphous stishovite may be much more rapid and accompanied by an appreciable volume reduction which decreases the Gibbs energy of the system under pressure. This explains why crystalline quartz becomes amorphous under pressure but does not explain why the transformation only occurs along some crystallographic planes. The dynamic aspect of a shock compression must play a fundamental role in the formation of these straight and narrow PDFs.

A shock compression is an irreversible process which is achieved by the propagation at supersonic velocity of a sharp and strong discontinuity of pressure and other thermodynamic quantities like temperature and specific volume. The moving shock front separates a region behind it which is uniformly and highly compressed (and in motion) from a region in front of it which still is at rest and uncompressed. The shock front is thus a sharp boundary separating two crystal lattices with markedly different parameters (for strong shock waves the lattice parameters of the compressed region can be reduced by up to 10%). The elastic energy due to such a misfit in the boundary is huge. In a static configuration it would be relaxed by misfit dislocations like the ones occurring in semi-conductor heterostructures for instance. This relaxation process does not hold, however, for a boundary moving at supersonic velocity because the misfit dislocations would have to follow the boundary (in climb motion). It has been suggested by Goltrant *et al.* [89] that the nucleation of small domains of a denser (amorphous) phase may relax the misfit elastic energy of the boundary (Fig. 10). As the shock front moves, the amorphised domains grow and follow it in order to continuously relax the boundary between compressed and uncompressed regions. They leave PDFs in their wake. This process does not require atomic diffusion over large distances. Only some shuffling in the unit cell occurs (transformation of a regular array of corner sharing SiO_4 tetrahedra in an irregular array of edge sharing SiO_6 octahedra). Goltrant *et al.* [89] also proposed a model for the nucleation of amorphous PDFs in quartz in the $\{10\bar{1}n\}$ planes based on a stability

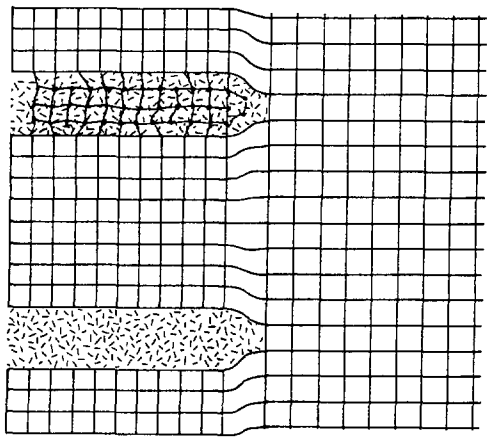

Fig. 10. — Formation mechanism of PDFs by the propagation of a shock wave front after [89].

criterion first proposed by Born [90,91]. This criterion states that a crystal elastically deformed is stable as long as its elastic energy is positive whatever the sign of the increment of elastic deformation (for instance in simple shear strain the shear modulus has to be positive). Goltrant *et al.* computed the shear modulus of quartz (considered as an anisotropic elastic medium) as a function of the confining pressure for a number of shear systems (shear plane $(hkil)$ and shear direction $[uvwt]$ in this plane). They used the data of Purton *et al.* [92] who computed from the first principles the variation with pressure (at zero K) of the components of the elastic stiffness tensor. They showed that the shear modulus of quartz becomes negative above a value $P \approx 10$ GPa for shear in the $[2\bar{1}\bar{1}0]$ direction and in the $\{01\bar{1}n\}$ planes with n values close to 1/2, 1, 2, 3, and 4. There is thus a correct quantitative agreement between this model and the experimental results.

PDFs in the basal plane represent a special case. They have been characterized as thin (20 to 100 nm) lamellae of Brazil twins. In Section 2, Brazil twins were described as grown-in defects with rhombohedral $\{10\bar{1}1\}$ habit planes. Such twins change the chirality of the crystal (left handed quartz $P3_121 \leftrightarrow$ right handed quartz $P3_221$). The thin Brazil twin lamellae induced by shock waves have a different habit plane (basal plane) and contain numerous $\mathbf{a}/2$ partial dislocations in their boundaries (Fig. 11). McLaren *et al.* [78] (see also Refs. [11] and [76]) proposed a few years ago a microscopic model for mechanical twinning in the basal plane. It would be induced by a large differential stress and would result from the cooperative glide of $\mathbf{a}/2$ partial dislocations in the basal plane. This strongly suggests that the actual thin basal twins are mechanical ones. This also suggests that the compressive shock wave develops at some stage of its propagation large differential stresses (tentatively estimated ≥ 4 GPa). Finally it is to be mentioned that in rocks which suffered a long and severe weathering after a meteorite impact event, most PDFs are recrystallized excepted these twin lamellae which appear as the most resistant shock signature at a microscopic scale. They are the only typical defects still unambiguously detected by TEM in rocks from very old meteorite craters like the Vredefort structure in South Africa or the Sudbury one in Canada, both being approximately two billion years old and the oldest meteorite craters detected so far on the Earth surface.

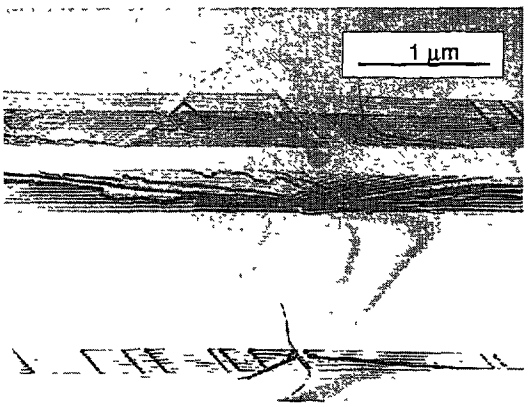

Fig. 11. — Thin basal twin lamellae produced by a shock wave. On this TEM micrograph they are inclined and their boundaries are outlined by a fringe system; partial **a** dislocations are visible in their boundaries.

6. Quartz in Industry; Piezoelectric Applications

When a load is applied on a piezoelectric material, electric charges appear on its surfaces: this is the direct piezoelectric effect. The inverse piezoelectric effect is the occurrence of a spontaneous deformation when an electric field is applied to a piezoelectric sample. These effects are described by equations (8a) and (8b) respectively

$$\mathbf{P} = \mathbf{d} : \boldsymbol{\sigma} = \mathbf{e} : \boldsymbol{\epsilon} \tag{8a}$$

and

$$\boldsymbol{\epsilon} = \mathbf{E}.\mathbf{d} \text{ or } \boldsymbol{\sigma} = \mathbf{E}.\mathbf{e} \tag{8b}$$

where $\mathbf{E}$ and $\mathbf{P}$ are the electric field and polarisation vector respectively, $\boldsymbol{\sigma}$ and $\boldsymbol{\epsilon}$ the usual second rank stress and strain tensors, and $\mathbf{d}$ and $\mathbf{e}$ the third rank deformation and stress piezoelectric tensors respectively. For a non piezoelectric material the usual Hooke's law of elasticity is

$$\boldsymbol{\sigma} = \mathbf{c} : \boldsymbol{\epsilon} \text{ or } \boldsymbol{\epsilon} = \mathbf{s} : \boldsymbol{\sigma} \tag{9}$$

$\mathbf{c}$ and $\mathbf{s}$ are the fourth rank stiffness and compliance tensors respectively. In a piezoelectric material the total deformation is the sum of its elastic and piezoelectric parts and the Hooke's law is to be written

$$\boldsymbol{\epsilon} = \mathbf{s} : \boldsymbol{\sigma} + \mathbf{E}.\mathbf{d} \tag{10}$$

By using the relevant Maxwell equations

$$\mathbf{D} = \epsilon_0 \mathbf{E} + \mathbf{P} \text{ and } \mathbf{P} = \epsilon_0 \boldsymbol{\chi}.\mathbf{E} \tag{11}$$

with ϵ_0 is the permitivity of vacuum and $\boldsymbol{\chi}$ is the second rank dielectric susceptibility tensor, the total polarisation is

$$\mathbf{P} = \mathbf{d} : \boldsymbol{\sigma} + \epsilon_0 \boldsymbol{\chi}.\mathbf{E} \text{ or } \mathbf{D} = \mathbf{d} : \boldsymbol{\sigma} + \boldsymbol{\chi}'.\mathbf{E} \text{ (with } \boldsymbol{\chi}' = 1 + \epsilon_0 \boldsymbol{\chi}) \tag{12}$$

Piezoelectricity is thus described by equations (10) and (12) or equivalently by

$$\boldsymbol{\sigma} = \mathbf{c} : \boldsymbol{\epsilon} - \mathbf{E}.\mathbf{e} \tag{13a}$$

and

$$\mathbf{D} = \mathbf{e} : \boldsymbol{\epsilon} + \boldsymbol{\chi}'.\mathbf{E} \tag{13b}$$

Let us now consider a piezoelectric specimen with parallel faces submitted to an alternative potential difference $V = V_0 e^{i\omega t}$ and let us look for the steady state electro-acoustic waves propagating in it. An electro-acoustic wave is described by a displacement vector $\mathbf{u}$ and an electric potential ϕ or equivalently by a quadri-vector (u_1, u_2, u_3, ϕ). The following equations are to be satisfied

$$\begin{array}{ll} - \text{ electric equations} & \text{div } \mathbf{D} = 0 \text{ and } \mathbf{E} = -\text{grad } \phi \\ - \text{ mechanical equations} & \boldsymbol{\epsilon} = \text{Def } \mathbf{u} \text{ or } \epsilon_{ij} = \frac{1}{2}\left(\frac{\partial u_i}{\partial x_j} + \frac{\partial u_j}{\partial x_i}\right) \\ - \text{ piezoelectric equations} & \boldsymbol{\sigma}.\mathbf{c} : \boldsymbol{\epsilon} - \mathbf{e}.\mathbf{E} \text{ and } \mathbf{D} = \mathbf{e} : \boldsymbol{\epsilon} + \boldsymbol{\chi}'.\mathbf{E} \\ - \text{ dynamic equations} & \text{Div } \boldsymbol{\sigma} = \rho \ddot{\mathbf{u}} \end{array} \tag{14}$$

where ρ is the specific mass. After some computations one obtains four equations

$$\sum_{i,k,l} c_{ijkl} \frac{\partial^2 u_k}{\partial x_l \partial x_i} - \sum_{n,l} e_{nij} \frac{\partial^2 \phi}{\partial x_n \partial x_i} = -\rho \omega^2 u_j \quad (j = 1 \text{ to } 3)$$

and

$$\sum_{i,l} e_{ikl} \frac{\partial^2 u_k}{\partial x_l \partial x_i} + \sum_{n,l} \frac{\partial^2 \phi}{\partial x_n \partial x_i} = 0 \tag{15}$$

These equations have a number of non trivial solutions which correspond to various modes of vibration (tilt, twist, ..). In general these solutions are complex functions of the components of the stiffness tensor c_{ijkl} and of the electromechanical coupling tensor e_{mnp}. All these coefficients vary with temperature T and in general the resonance frequency $1/\tau = 2\pi/\omega$ also varies with T. There exists, however, a few piezoelectric materials with the remarkable property of having a few crystalline orientations such that the temperature variations of c_{ijkl} and e_{mnp} precisely compensate in a relatively large temperature range and the resonance frequency $1/\tau$ becomes practically independent of temperature variations. This is the case for quartz, berlinite $AlPO_4$, and lithium tantalate $LiTaO_3$. Resonators for clocks are made with thin quartz lamellae cut parallel to one of these orientations. In contrast electronic thermometers are based on the measurement of the frequency shift of quartz resonators cut with an orientation presenting a large sensitivity to temperature variations.

Progress in time keeping accuracy requires that the electro-mechanical waves are not disturbed by physical defects. The thin metallic electrodes (generally gold) deposited on the surfaces induce elastic stresses in the vibrating quartz lamella. These stresses seem to slightly decrease with time (relaxation by dislocation reorganisation, .) and the resonance frequency also slightly vary with time (ageing phenomenon). Dislocations in the quartz lamella also decrease the quality factor of the resonator because they scatter the electro-acoustic waves. However, small amounts of water (tiny inclusions or water point defects) remain actually the limiting defects in standard material. The numerous tiny water inclusions present in the synthetic quartz grown in the sixties limited their quality factor to values of the order of $Q \approx 10^5$. In recently grown high quality crystals one generally assumes that the concentration of $(4H)_{Si}$ and/or Al-OH point defects still are the factor limiting the performances. The effect of these point defects can be understood as follows. The electro-acoustic wave produces a periodic deformation. The proton environment of the $(4H)_{Si}$ and Al-OH defects is also modified. This changes the stable sites of the protons which thus continuously jump from a position to another one. There is however a phase shift between acoustic wave and proton vibrations and, as a

result there is a loss of electro-acoustic energy (internal friction). The quality factor Q of a resonator is measured by the ratio of the maximum energy reached during a cycle divided by the energy loss during this cycle. Q reaches 4 to 5×10^6 for premium grade resonators with no detectable OH and very small Al content. This premium grade quartz may be improved by a long electro-diffusion process at a temperature just below the $\alpha - \beta$ transition and an electric field of $\approx$ 1,000 V/cm. It is generally assumed that this process still decreases the water content of the crystal. It might also decrease its Al and/or Na content.

7. Conclusion

Since the discovery of the hydrolytic weakening of quartz in 1965 our knowledge of its micro-mechanisms has considerably progressed and the general concepts are now correctly understood. There remains however a number of problems imperfectly solved. The equilibrium solubility and the diffusivity of water point defects are not well known. Models of the water assisted glide motion of dislocations still are very crude as compared with the models developed for covalent semi-conductors for instance. There still is no reliable creep law for wet quartz taking into account the parameter "water content" which could be extrapolated to the very low strain rates and low stresses of natural deformation in the Earth's crust. Hydrolytic weakening also occurs in other silicate minerals but the understanding of the associated micro-mechanisms has not received much attention. The micro-mechanism of amorphisation of quartz (and other silicates) under shock is not well understood. Finally it can be said that the industrial applications of quartz have reached a high degree of perfection but there still is a need for better and purer crystals.

References

[1] Griggs D.T. and Blacic J.N., Quartz: anomalous weakness of synthetic crystals, *Sci.* **147** (1965) 292-295.

[2] Griggs D.T., Hydrolytic weakening of quartz and other silicates, *Geophys J. R. Astr. Soc.* **14** (1967) 19-31.

[3] Griggs D.T., A model of hydrolytic weakening in quartz, *J. Geophys. Res.* **79** (1974) 1653-1661.

[4] Carter N.L., Christie J.M. and Griggs D.T., Experimental deformation and recrystallisation of quartz, *J. Geol.* **72** (1964) 687-733.

[5] Christie J.M., Griggs D.T. and Carter N.L., Experimental evidence of basal slip in quartz, *J. Geol.* **72** (1964) 734-756.

[6] Blacic J.D. and Christie J.M., Plasticity and hydrolytic weakening of quartz single crystals, *J. Geophys. Res.* **89** (1984) 4223-4239.

[7] Kronenberg A.K., Hydrogen speciation and chemical weakening of quartz, In "Reviews in Mineralogy" (P.J. Heaney and C.T. Prewitt, Eds) Min. Soc. Amer. (1994) pp. 123-176.

[8] Baeta R.D. and Ashbee K.H.G., Slip systems in quartz; I Experiments, *Amer. Mineral.* **54** (1969) 1551-1566.

[9] Baeta R.D. and Ashbee K.H.G., Mechanical deformation of quartz. I Constant strain rate compression experiments, *Phil. Mag.* **22** (1970) 601-624.

[10] Linker M.F. and Kirby S.H., Anisotropy in the rheology of hydrolytically weakened synthetic quartz crystals. In "Mechanical behaviour of crustal rocks" (N.L. Carter, M. Friedman, J.M. Logan and D.W. Stearns, Eds.) Geophys. Monograph 24 Amer Geophys Union (Washington, 1981) pp. 29-48.

[11] Doukhan J.C. and Trépied L., Plasticity of quartz, crystallographic models and TEM observations, *Bull. Minéral.* **102** (1979) 159-172.

[12] Doukhan J.C. and Trépied L., Plastic deformation of quartz single crystals, *Bull. Minéral.* **108** (1985) 97-123.

[13] Karato S., Paterson M.S. and FitzGerald J.D., Rheology of synthetic olivine aggregates: influence of grain size and water, *J. Geophys. Res.* **91** (1986) 8151-8176.

[14] Ross J.V., and Nielsen K.C., High temperature flow of wet polycrystalline enstatite, *Tectonophys* **44** (1978) 233-261.

[15] Boulogne B., François P., Cordier P., Doukhan J.C., Philippot E. and Jumas J.C., Plastic deformation of wet synthetic α berlinite $AlPO_4$, *Phil. Mag. A* **57** (1988) 411-430.

[16] McLaren A.C. and Retchford J.A., TEM study of the dislocations in plastically deformed synthetic quartz, *Phys. Stat. Sol.* **33** (1969) 657-668.

[17] Hirsch P.B., Plastic deformation and electronic mechanisms in semi-conductors and insulators, *J. Phys. C* **31** (1981) 49-160.

[18] Hobbs B.E., The influence of metamorphic environment upon the deformation of minerals, *Tectonophys.* **78** (1981) 335-383.

[19] Hobbs B.E., The hydrolytic weakening effect in quartz, In "Point defects in minerals" (R.N. Schock, Ed.) Geophys Monogr 31, Amer Geophys Union (Washington, 1985) pp. 151-170.

[20] Alexander H. and Haasen P., Dislocations and plastic flow in the diamond structure, *Solid State Phys.* **22** (1968) 27-158.

[21] Heggie M., The structure of dislocations, principally in silicon, inferred from experimental and theoretical results, In "Dislocations" P. Veyssiere, L. Kubin, Eds (Editions du CNRS, 1984) pp. 305-314.

[22] Heggie M. and Nylen M., Dislocations core structures in α quartz derived from a valence force potential, *Phil. Mag.* **50** (1984) 543-555.

[23] Heggie M. and Nylen M., Dislocations without deep states in α quartz, *Phil. Mag.* **51** (1985) L69-L72.

[24] Brice J.C., Crystals for quartz resonators, *Rev. Modern Phys.* **57** (1985) 105-146.

[25] Laudise R.A. and Barns R.L., Perfection of quartz and its connection to crystal growth, *IEEE Trans on Ultrasonics, Ferroelectrics, and Frequency Control* **35** (1988) 277-287.

[26] Besson R.J., Recent evolution and new developments of piezoelectric resonators, Proceedings of the 2nd European Time and Frequency Forum (1989) pp. 921-936.

[27] Bragg W. and Gibbs R.E., The structure of α and β quartz, *Roy. Soc. Proc.* **59** (1926) 405-427.

[28] Frank F.C., On Miller-Bravais indices and four dimensional vectors, *Acta Cryst.* **18** (1965) 862-866.

[29] Nicholas J.F., The indexing of hexagonal crystals, *Phys. Stat. Sol. (a)* **1** (1970) 563-571.

[30] Halliburton L.E., Martin J.J. and Koeler D.R., Properties of piezoelectric materials. In "Precision Frequency Control", vol 1, E.A. Gerber and A. Ballato Eds (Academic press, 1985) pp. 1-45.

[31] Frondel C., Dana's system of mineralogy (J Wyley Ed., New York, (1962).

[32] Barns R.L., Freeland P.E., Kolb A. and Patel J.R., Dislocation free and low dislocation quartz prepared by hydrothermal crystallisation, *J. Cryst. Growth* **43** (1978) 676-686.

[33] Gratz A.J., Manne S. and Hansma P.K., Atomic force microscopy of atomic-scale ledges and etch pits formed during dissolution of quartz, *Sci.* **251** (1991) 1343-1346.

[34] Lang A.R. and Muiskov V.F., Dislocations and fault surfaces in synthetic quartz, *J. Appl. Phys.* **38** (1967) 2477-2483.

[35] McLaren A.C., Osborne C.F.F. and Saunders L.A., X-ray topographic study of dislocations in synthetic quartz, *Phys. Stat. Sol. (a)* **4** (1971) 235-247.

[36] Ser A., Bideau J.P., Clastre J. and Zarka A., Etude des défauts de croissance dans des monocristaux naturels de quartz, *J. Appl. Cryst.* **13** (1980) 50-57.

[37] Ardell A.J., Christie J.M. and McCormick J.W., Dislocation images in quartz and the determination of Burgers vectors, *Phil. Mag.* **29** (1974) 1399-1411.

[38] Trépied L. and Doukhan J.C., Evidence of $< \mathbf{a} + \mathbf{c} >$ dislocations in synthetic quartz single crystals compressed along the **c** axis, *Bull. Minéral.* **105** (1982) 176-180.

[39] Cordier P., Morniroli J.P. and Cherns D., Characterization of crystal defects by Large Angle Convergent-Beam Electron Diffraction (LACBED), *Phil. Mag.* (1995, in press).

[40] Trépied L. and Doukhan J.C., Dissociated **a** dislocations in quartz, *Phys. Stat. Sol. (a)* **49** (1978) 713-724.

[41] Cherns D., Hutchison J.L., Jenkins M.L. and Hirsch P.B., Electron irradiation induced vitrification at dislocations in quartz, *Nature* **287** (1980) 314-316.

[42] Cordier P. and Doukhan J.C., Plasticity and dissociation of dislocations in water-poor quartz *Phil. Mag.* (1995) in press.

[43] Paterson M.S., The determination of hydroxyl by infrared absorption in quartz, silicate glasses and similar materials, *Bull. Minéral.* **105** (1982) 20-29.

[44] Aines R.D., Kirby S.H. and Rossman G.R., Hydrogen speciation in synthetic quartz, *Phys. Chem. Minerals.* **11** (1984) 204-212.

[45] Aines R.D. and Rossman G.R., Water in minerals? A peak in the infrared, *J. Geophys. Res.* **89** (1984) 4059-4071.

[46] McLaren A.C., Cook R.F., Hyde S.T. and Tobin R.C., The mechanisms of the formation and growth of water bubbles and associated dislocation loops in synthetic quartz, *Phys. Chem. Minerals.* **9** (1983) 79-94.

[47] Halliburton L.E., Koumvalis N., Markes M.E. and Martin J.J., Radiation effects in crystalline SiO_2, the role of aluminum, *J. Appl. Phys.* **52** (1981) 3565-3574.

[48] Kronenberg A.K., Kirby S.H., Aines R.D. and Rossman G.R., Solubility and diffusional uptake of hydrogen in quartz at high water pressures: implications for hydrolytic weakening, *J. Geophys. Res.* **91** (1986) 12723-12744.

[49] Rovetta M.R., Holloway J.R. and Blacic J.N., Solubility of hydroxyl in natural quartz annealed in water at 900 °C and 1.5 GPa, *Geophys. Res. Lett.* **13** (1986) 145-148.

[50] Gerretsen J., Paterson M.S. and McLaren A.C., The uptake and solubility of water in quartz at elevated pressure and temperature, *Phys. Chem. Minerals.* **16** (1989) 334-342.

[51] Mackwell S.J. and Paterson M.S., Water related diffusion and deformation effects in quartz at pressures of 1500 and 300 MPa. In "Point defects in minerals" (R.N. Schock, Ed.) Geophys Monograph 31, Amer Geophys Union (Washington, 1985) pp. 141-150.

[52] Doukhan J.C. and Paterson M.S., Solubility of water in quartz, a revision, *Bull. Mineral.* **109** (1986) 193-198.

[53] Paterson M.S., The thermodynamics of water in quartz, *Phys. Chem. Minerals.* **13** (1986) 245-255.

[54] Cordier P., Boulogne B. and Doukhan J.C., Water precipitation and diffusion in wet quartz and wet berlinite $AlPO_4$, *Bull. Minéral.* **111** (1988) 113-137.

[55] Rovetta M.R., (1989) Experimental and spectroscopic constraints on the solubility of hydroxyl in quartz, *Phys. Earth Plan. Int.* **55** (1989) 326-334.

[56] Cordier P. and Doukhan J.C., Water in quartz, solubility and influence on ductility, *Eur. J. Mineral.* **1** (1989) 221-237.

[57] Cordier P. and Doukhan J.C., Water speciation in quartz; a near infrared study, *Amer. Miner.* **76** (1991) 361-369.

[58] Haggon J.P., Stoneham A.M. and Jaros M., Transport processes in silicon oxidation. I Dry oxidation, *Phil. Mag. B* **55** (1989) 211-224; II wet oxidation, *Phil. Mag. B* **55** 225-235.

[59] Cohen-Addad C., Ducros P. and Bertaut E.F., Etude de la substitution du groupement SiO_4 par $(OH)_4$ dans les composés $Al_2Ca_3(OH)_{12}$ et $Al_2Ca_3(SiO_4)_{2,16}$ $(OH)_{3,36}$ de type grenat, *Acta Cryst.* **23** (1967) 220-230.

[60] Basso R., Della-Gusta A. and Zefiro L., Crystal structure refinement of plazolite: a highly hydrated natural hydrogrossular, *N. Jb. Miner. Mh.* **H6** (1983) 251-258.

[61] Lager G.A., Ambruster Th. and Faber J., Neutron and X-ray diffraction study of hydrogarnet $Ca_3Al_2(O_4H_4)_3$, *Am. Mineral.* **72** (1987) 756-765.

[62] Nutall R.H.D. and Weil J.A., Two hydrogenic trapped hole species in α-quartz, *Solid State Com.* **33** (1980) 92-102.

[63] Weil J.A., A review of electron spin spectroscopy and its application to the study of paramagnetic defects in crystalline quartz, *Phys. Chem. Minerals* **10** (1984) 149-165.

[64] Cordier P., Weil J.A., Howarth D.F. and Doukhan J.C., Influence of $(4H)_{Si}$ defects on dislocation motion in quartz, *Eur. J. Miner.* **5** (1994) 17-23.

[65] Burnham C.W., Holloway J.R. and Davis N.F., Thermodynamic properties of water to 1,000 °C and 10,000 bars, Geol Soc Am Sp Paper (Washington, 1969) pp. 132-152.

[66] Barin I. and Knacke O., Thermochemical properties of inorganic substances, Springer Verlag (Berlin, 1973) p. 323-326.

[67] Halbach H. and Chaterjee N.D., An empirical Redlich-Kwong-type equation of state for water to 1,000 °C and 200 kbars, *Contrib. Miner. Petrol.* **79** (1982) 337-345.

[68] Ord A. and Hobbs B.E., Experimental control of the water-weakening effect in quartz, In "Mineral and rock deformation: laboratory studies". (B.E. Hobbs and H.E. Heard, Eds) Geophys Monograph 36, Amer Geophys Union (Washington, 1986) pp. 51-72.

[69] Bartholomew R.F., Butlerb L., Hoover H.L. and Wu C.K., Infrared spectra of water containing glass, *J. Amer. Ceram. Soc.* **63** (1980) 481-485.

[70] Stone J.G. and Walrafen E.D., Overtone vibrations of OH groups in fused silica optical fibers, *J. Chem. Phys.* **76** (1982) 1712-1727.

[71] Stopler E., Water in silicate glasses: an infrared spectroscopic study, *Contrib. Mineral. Petrol.* **81** (1982) 1-17.

[72] Langer K. and Flörke O.W., Near infrared absorption spectra (4000-9000 cm^{-1}) of opals and the role of water in these $SiO_2.nH_2O$ minerals, *Fort. Mineral.* **16** (1974) 334-342.

[73] Flörke O.W., Kohler-Herbertz B. and Tonges I., Water in microcrystalline quartz of volcanic origin: Agates, *Contrib. Mineral. Petrol.* **80** (1982) 324-333.

[74] Hobbs B.E., McLaren A.C. and Paterson M.S., Plasticity of single crystals of synthetic quartz. In "Flow and fracture of rocks" (H.C. Heard, I.Y. Borg, N.L. Carter and C.B. Raleigh Eds), Geophys Monograph 16, Amer Geophys Union (Washington, 1972) pp. 29-53.

[75] Paterson M.S. and Kekulawala K.R.S.S., The role of water in quartz deformation, *Bull. Minéral.* **102** (1979) 92-100.

[76] Kekulawala K.R.S.S., Paterson M.S. and Boland J.N., An experimental study of the role of water in quartz deformation. In "Mechanical behaviour of crustal rocks" (N.L. Carter, M. Fridman, J.M. Logan and D.W. Stearns Eds) Geophys Monograph 24, Amer Geophys Union (Washington, 1981) pp. 49-60.

[77] Baldermann M., The effect of strain rate and temperature on the yield point of hydrolytically weakened synthetic quartz, *J. Geophys. Res.* **79** (1974) 1647-1652.

[78] Christie J.M. and Ardell A.J., Deformation structures in minerals. In "Electron Microscopy in Mineralogy", (R. Wenk Ed, Springer Verlag (Berlin, 1976) pp. 374-403.

[79] McLaren A.C., Retchford J.A., Griggs D.T. and Christie J.M., TEM study of Brazil twins and dislocations experimentally produced in natural quartz, *Phys. Stat. Sol.* **19** (1967) 631-644.

[80] Heggie M., A molecular water pump in quartz, dislocations, *Nature* **355** (1992) 337-338.

[81] Ball A. and Glover G., Dislocation climb deformation in quartz, *Bull. Minéral.* **102** (1979) 188-194.

[82] Kirby S.H. and McCormick J.W., Creep of hydrolytically weakened synthetic quartz crystals oriented to promote $[2\bar{1}\bar{1}0] < 0001 >$ slip; a brief summary of work to date, *Bull. Minéral.* **109** (1979) 124-137.

[83] McLaren A.C., FirzGerald J.D. and Gerresten J., Dislocation nucleation and multiplication in synthetic quartz: relevance to water weakening, *Phys. Chem. Minerals.* **16** (1989) 465-482.

[84] Morrison-Smith D.J., Paterson M.S. and Hobbs B.E., TEM study of plastic deformation in single crystals of synthetic quartz, *Tectonophys.* **33** (1976) 43-79.

[85] Kekulawala K.R.S.S., Paterson M.S. and Boland J.D., Hydrolytic weakening in quartz, *Tectonophys.* **46** (1978) T1-T6.

[86] Koch P.S., Christie J.M., Ord A. and George R.P., Effect of water on the rheology of experimentally deformed quartzite, *J. Geophys. Res.* **94** (1989) 13,975-13,996.

[87] FitzGerald J.D., Boland J.N., McLaren A.C., Ord A. and Hobbs B.E., Microstructures in water-weakened single crystals of quartz, *J. Geophys. Res.* **96** (1991) 2139-2155.

[88] Gratz A.J., Nellis W.J., Christie J.M., Brocius W., Swegle J. and Cordier P., Shock metamorphism of quartz with initial temperatures -170 to 1000 °C, *Phys. Chem. Minerals.* **19** (1992) 267-288.

[89] Goltrant O., Leroux H., Doukhan J.C. and Cordier P., Formation mechanisms of planar deformation features in naturally shocked quartz, *Phys. Earth Planet Int.* **74** (1992) 219-240.

[90] Born M., Thermodynamics of crystals and melting, *J. Chem. Phys.* **7** (1939) 591-603.

[91] Born M. and Huang K., Dynamical theory of crystal lattices, Oxford University Press (London, 1954).

[92] Purton J., Jones R., Catlow C.R.A. and Leslie M., Ab-initio potentials for the calculation of the dynamical and elastic properties of α-quartz, *Phys. Chem. Minerals.* **19** (1993) 392-400.